

Determination of the $2p$ - $1s$ transition energy and strong interaction shift in pionic hydrogen using crystal diffraction

A. Forster, E. Bovet,* J. Gimlett, H. E. Henrikson, D. Murray,[†] R. J. Powers, P. Vogel, and F. Boehm
California Institute of Technology, Pasadena, California 91125

R. Kunselman

University of Wyoming, Laramie, Wyoming 82071

P. L. Lee

California State University of Northridge, Northridge, California 91330

(Received 29 July 1983)

The $2p$ - $1s$ atomic transition in pionic hydrogen has been studied with the help of a point-focusing graphite diffraction spectrometer. The transition energy was measured to be $E(2p-1s)=2433.5\pm 1.7$ eV. From this result a strong interaction shift of -3.9 ± 1.7 eV was derived. The $K\alpha$ x-ray yield in the 2.7 atm hydrogen target at 40 K was found to be 0.025 ± 0.013 per stopped pion.

I. INTRODUCTION

Pionic hydrogen, an elementary atomic system composed of a bound proton and a π^- , is an attractive source of information for the study of the strong interaction between the proton and the pion. The strong interaction manifests itself mainly while the pion resides in the atomic $1s$ level before being absorbed by the nucleus, and produces a shift in energy as well as an increase in the width of the $2p$ - $1s$ atomic transition.

In the absence of the strong interaction, the $2p$ - $1s$ transition energy can be calculated to a sufficiently high precision as the sum of the energy eigenvalue of the Klein-Gordon Hamiltonian of a particle in a Coulomb field and a term to account for vacuum polarization. The strong interaction shift is the difference between this calculated value and the experimentally measured energy.

From an experimental point of view, it is difficult to determine the strong interaction shift accurately because the low event rate, the small size of the energy shift, and the low absolute x-ray energy place demanding, and somewhat conflicting, requirements on the instrumental efficiency and energy resolution.

Previous studies^{1,11} using a gas proportional counter have provided some guidance as to the magnitude of the effect. The purpose of the present study was to improve the accuracy of the value of the strong-interaction shift employing a crystal-diffraction technique. A point-focusing graphite crystal spectrometer has been built for this purpose.¹

In Sec. II we describe this spectrometer and the experimental conditions under which the experiment was carried out. In Sec. III we discuss our results and compare them with data from low-energy pion-proton scattering.

II. EXPERIMENTAL TECHNIQUE

The experimental apparatus consists of three main parts: the hydrogen target where the pionic $2p$ - $1s$ x rays

are produced, the diffraction crystal, and the radiation detector. To minimize x-ray absorption, the apparatus was enclosed in a container filled with He gas. Figure 1 illustrates the position of the apparatus with respect to the pion beam line. Target and beam line were separated from the spectrometer crystal and detector by 135 cm of high density concrete and polyethylene. The experiment was performed at the east cave of the stopped muon channel (SMC) at the Los Alamos Meson Physics Facility (LAMPF). The linear accelerator was typically operating with proton beams of $600 \mu\text{A}$.

Figure 2 depicts the target cryostat. Hydrogen gas at a pressure of 2.7 atm was contained in an aluminum vessel thermally isolated by a vacuum jacket and several layers of superinsulation. The target vessel was cooled to 40 K by means of a closed cycle refrigerator. Temperature sensors (Si diodes) monitored the temperature throughout the experiment. The x rays exited the target cell through two Mylar windows reinforced by a Cu-Be mesh, one at the target cell and the other at the outer vacuum jacket. The total transmission of these two windows is 26% at 2.5 keV. A 12.5 cm thick polyethylene degrader attached to the target cell served to slow down the π^- beam so as to optimize the pion stopping rate and thus the x-ray yield in the target.

The target cell was positioned 60 cm away from the focal point of the spectrometer in order to allow for more shielding between target and detector. A collimator $25\times 25 \text{ mm}^2$ at the focal point defines an entrance window optimized with respect to the mosaic spread of the diffraction crystal. This arrangement had an additional advantage of accepting radiation from nearly the entire illuminated target volume. Therefore, a uniform profile was obtained across the entrance window in the focal plane.

After passing through the collimator (see Fig. 1) the x-ray beam impinges on the point-focusing graphite diffraction crystal. The crystal, described in detail in Ref. 1, consists of an array of $20 \text{ } 12\times 100 \text{ mm}^2$ and 0.1 mm thick

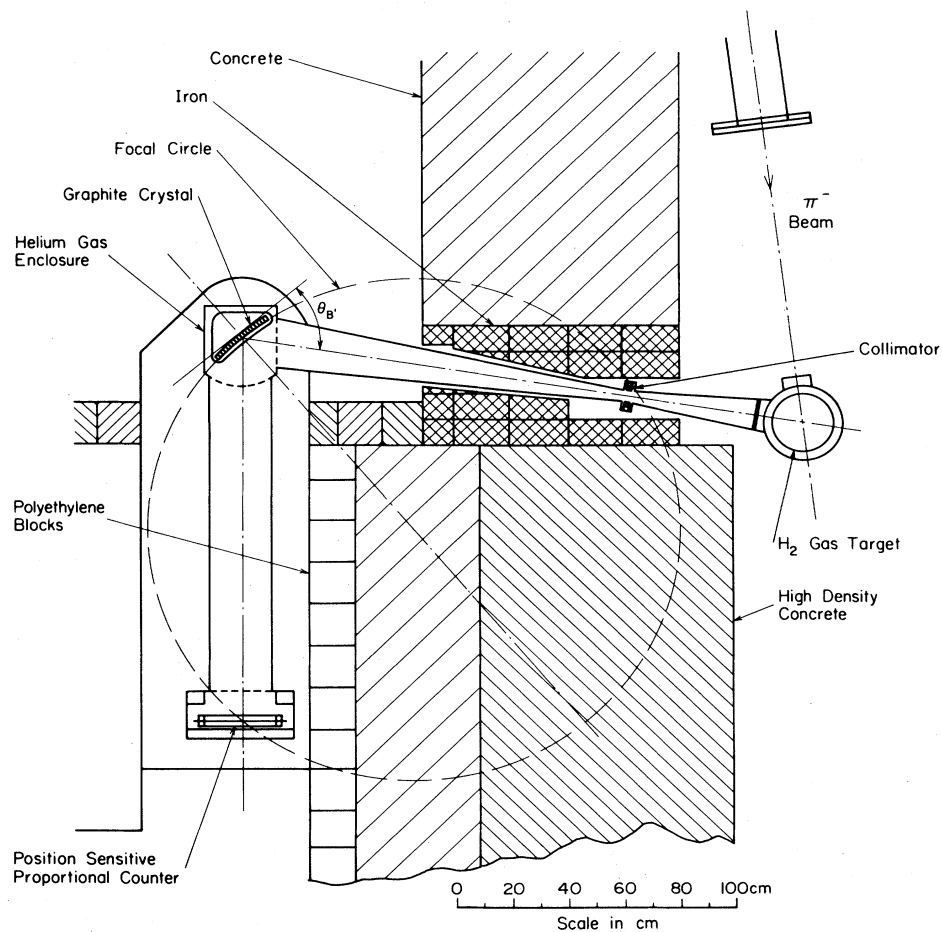


FIG. 1. Experimental setup at the LAMPF stopped muon channel. The instrument is surrounded by a concrete cave.

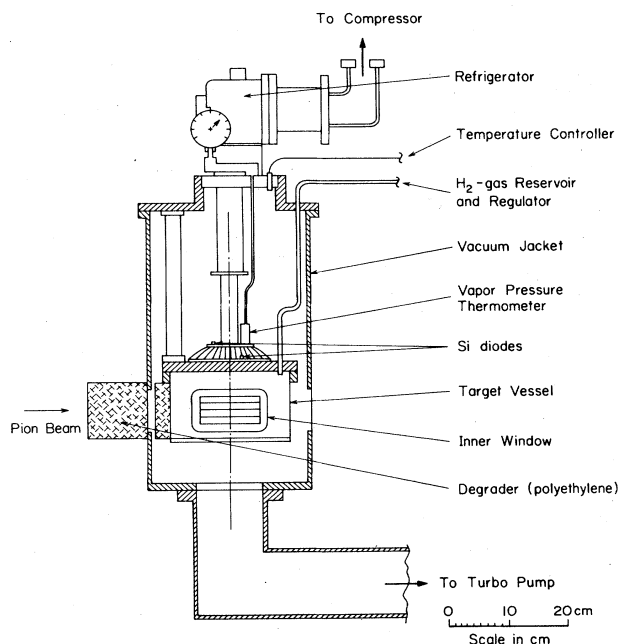


FIG. 2. Cryostat for the H_2 target.

sheets of graphite crystal, each supported by a backing mounted along the focal circle and satisfying the Bragg condition for a point source.² Vertical focusing was achieved by vertical curvature of the sheets. The crystal arrangement could be rotated about an axis perpendicular to the focal plane in a range from about 43 to 51 deg with reference to the center of the target. The accuracy of this motion was better than 5 s of arc.

The (002) reflecting planes in graphite have a lattice spacing of $d = 3.355 \text{ \AA}$.^{3,4} A value of 3.3×10^{-2} was determined earlier¹ for the reflectivity for 2.6 keV photons.

The diffracted x rays entered a position-sensitive proportional counter¹ (PSPC), 20 cm long and 3.8 cm diam, operating with a continuously flowing gas mixture of 90% Ar and 10% CH_4 at ambient pressure. The counter window was 0.7 mg/cm^2 polypropylene coated with graphite.

Figure 3 shows the electronics scheme for obtaining position information. The pulse rise times at the two ends of the counter wire are compared by means of two timing single channel analyzers (SCA's) and a time-to-amplitude converter (TAC) subject to an energy condition (sum pulse) which served as a gate pulse. Only events which deposited $2.4 \pm 0.3 \text{ keV}$ energy in the counter were re-

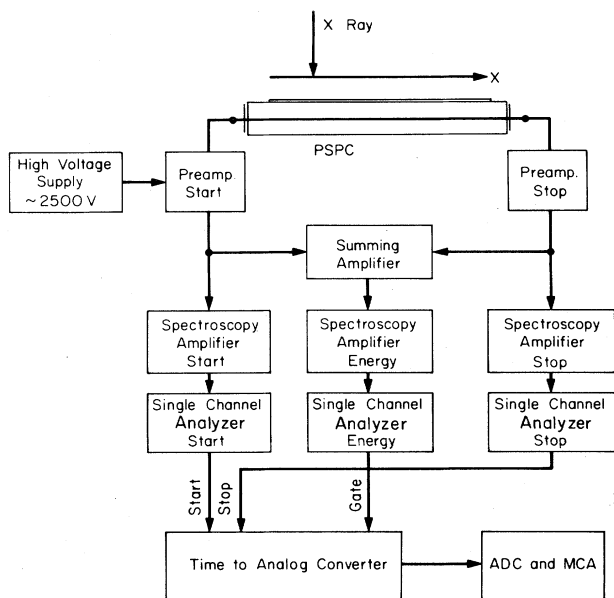
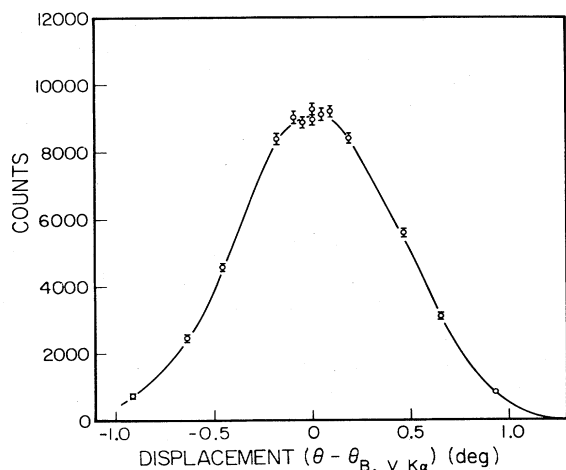
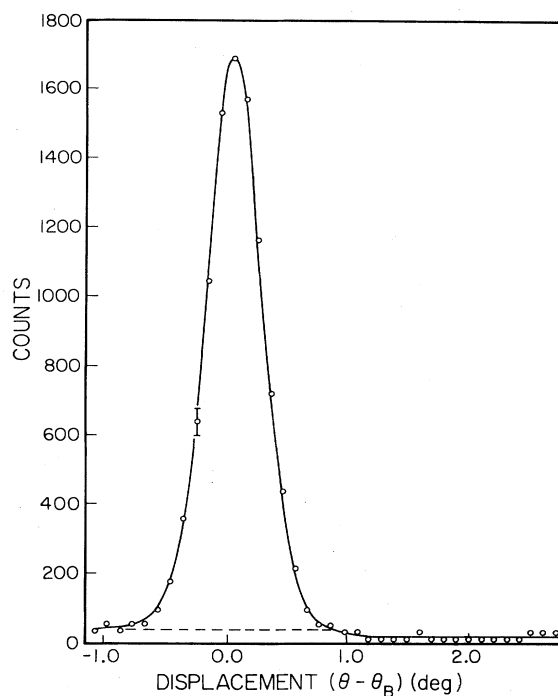


FIG. 3. Schematic of the readout electronics.

tained in the analysis. At a wire voltage of 1500 V the position resolution for a 2.5 keV x ray was better than 1 mm (0.08 eV). Good linearity over the active length of 200 mm was obtained by carefully matching the impedances of the counter and the preamplifiers. In the analysis the relationship between the TAC output voltage and the actual position, as obtained by means of a movable collimator slit, was expressed by a fifth order polynomial and reproduced this relationship within an accuracy of 0.1% over the entire range of the counter. The overall stability turned out to be within 0.02 eV during the experiment. The total transmission of the spectrometer system, defined as the ratio of the number of photons detected to the number of photons incident to the crystal from the target cell,

FIG. 4. Rocking curve of the graphite crystal for V $K\alpha$ x ray.FIG. 5. V $K\alpha_{1,2}$ calibration line.

was determined to be $(1.2 \pm 0.1) \times 10^{-6}$.

The spectrometer was calibrated with the help of several x-ray lines. A convenient calibration line is the V $K\alpha_1$ x ray at 2.50356 \AA^* ,⁵ corresponding to 4.9523 keV (Ref. 6) observed in second order, excited in a vanadium foil ($50 \times 25 \text{ mm}^2$) by radiation from a 10 mCi ^{55}Fe source. [It should be noted that, in relating first and second order reflexes in reflection geometry, a small refractive index correction⁷ must be applied. In the present situation (a Bragg angle of 48°) this correction amounts to a fractional change $\Delta E/E = 2 \times 10^{-5}$ and can be neglected.]

Figure 4 shows a rocking curve obtained in the following manner. With the vanadium source placed behind the collimator, the crystal was rotated through a range of angles near the Bragg angle. The integral response in the position sensitive detector was recorded for each angular setting. The centroid of the rocking curve (Fig. 4) determines the angular position of the crystal corresponding to the Bragg angle θ_B of V $K\alpha$ lines. With the crystal fixed at this position, the response of the position sensitive proportional counter was measured. For the vanadium line the position response is shown in Fig. 5 in angular units $(\theta - \theta_B)$ with respect to the centroid θ_B . The instrumental line width was found to be $0.50 \pm 0.05 \text{ deg}$ (19 eV), the broadening being due to the instrumental resolution of the graphite crystal spectrometer. Because of this instrumental broadening, the spectrometer will still transmit radiation with wavelengths differing slightly from that for the chosen Bragg condition.

The position sensitive proportional counter makes it possible to obtain a measurement of the entire x-ray pro-

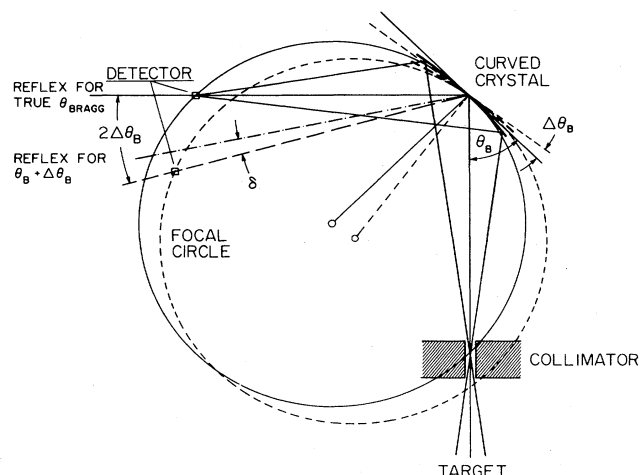


FIG. 6. Geometry of the crystal spectrometer. The solid lines show the optics for an angle setting θ_B (exact Bragg angle for a given energy); the dashed lines show the optics for an angle setting $\theta_B + \Delta\theta_B$.

file without rotating the crystal in the usual θ and 2θ mode. It should be kept in mind, however, that the observed centroid position corresponds to the Bragg angle only if the crystal is set at the true Bragg angle with respect to the fixed incident beam, as illustrated in Fig. 6. Suppose the crystal is set at an angle $\theta_B + \Delta\theta_B$ close to the yet unknown angle θ_B for the x ray to be measured. Owing to the instrumental broadening of the crystal, a diffracted line can be observed, but its position in the counter deviates from $\theta_B + 2\Delta\theta_B$ (this would be the position for a very narrow collimator) by an amount δ . This deviation δ arises from the folding of the intensity profile of the target with the transmission function of the spectrometer. For small offsets, it is proportional to $\Delta\theta_B$ and can be calculated from the optics of the spectrometer and measured, for example, for $V K\alpha$ radiation.

The procedure for obtaining the wavelength of an x-ray line is to measure δ for at least two "best guesses" of the crystal Bragg angle setting, $\theta_B + \Delta\theta_{B1}$ and $\theta_B + \Delta\theta_{B2}$. The true Bragg angle θ_B can now be obtained by linear interpolation to $\delta=0$ of the observed δ vs $\Delta\theta_B$ relation. The measured constant of proportionality is used to constrain the fit.

The described procedure was tested for the $S K\beta$ line. A sulfur target in an arrangement similar to that of the vanadium target was used. The observed energy of 2.4652 ± 0.0006 keV agrees well with the listed value of 2.4654 keV.^{5,8}

The intensity profile of the π^- beam entering the target cell was studied with the help of titanium sheets mounted at various positions inside the cell. The π^- Ti $4f$ - $3d$ x-ray intensity was measured with a Ge detector, positioned in place of the diffraction crystal, and the intensity was found to be constant within the accuracy of our measurement over the width of the cell (along the beam direction). It was concluded that any line shift associated with the spatial distribution of the pion beam is expected to be smaller than 0.1 eV.

From the x-ray intensity of the Ti target, we found the pion stop rate, using the known x-ray yield of 0.30 for the $4f$ - $3d$ transition in Ti (Ref. 9), to be $(1.0 \pm 0.1) \times 10^6$ s⁻¹ in a 0.36 g/cm² thick target for a 600 μ A proton current on the LAMPF production target A2. From a simple scaling model for the energy loss per unit length,¹⁰ we calculated the stop rate in a 0.011 g/cm² H₂ target (40 K, 2.7 atm) to be $(6.0 \pm 0.7) \times 10^4$ s⁻¹.

III. RESULTS AND DISCUSSION

Pionic hydrogen spectra were recorded for a total of 280 h for three settings of the crystal, as described above. An additional measurement with an evacuated target cell was performed in order to study the background. The data for two settings are displayed in Figs. 7(a) and (b). The fitted curves are a Gaussian superimposed on a quadratic background. The width of the Gaussian was taken from the $V K\alpha$ calibration lines (Fig. 5), whose small Lorentzian width (Fig. 5) of less than 1 eV and fine structure splitting were taken into account. No attempt was made to measure the strong-interaction broadening, which is expected to be small.^{11,13-15}

From the area under the x-ray line, and taking into account the spectrometer efficiency, we found the production rate of the $2p$ - $1s$ x rays in the target to be $(1.5 \pm 0.7) \times 10^3$ s⁻¹, from which a $K\alpha$ x-ray yield of $Y_{K\alpha} = 0.025 \pm 0.013$ per stopped pion is obtained.

This result can be compared with early measurements at 4 atm and 297 K by Bailey *et al.*¹¹ who report a value of $Y_K = 0.40 \pm 0.04$ for the total number of K x rays emitted per pion captured by the proton. From their branching ratio, $K\alpha/K = 0.53 \pm 0.04$, the corresponding number of $K\alpha$ x rays is $Y_{K\alpha} = 0.21 \pm 0.03$. Bailey *et al.* reported that more than 50% of the stopped pions decay ($\tau = 2.6 \times 10^{-8}$ s) before reaching the atomic $2p$ level. This claim, however, is difficult to reconcile with the short lifetime of about 10^{-10} s of the pionic cascade^{12,13} in the $\pi^- p$ atom.

The present result, expressed as the total K x-ray yield, is

$$Y_{\text{tot}} = Y_{K\alpha} / B = 0.06 \pm 0.03$$

with

$$B = Y_K / Y_{K_{\text{tot}}} = 0.45$$

(Ref. 13). This value, together with that of Ref. 11, is plotted in Fig. 8 as a function of target pressure (equivalent pressure at 297 K). The curves are calculations by Borie and Leon¹³ for several choices of the parameters, including the strength of the Stark mixing (STK), the kinetic energy T of the hydrogen atom, and the strong interaction shift ΔE_{1s} of the $1s$ level. The figure illustrates the acceptable range of parameters for both experiments. As can be seen, the two experimental results agree poorly with each other.

The transition energy was determined from the observed centroid employing the method outlined in the preceding section. A value of 2433.5 ± 1.7 eV was found.

Owing to the low x-ray yield and low spectrometer effi-

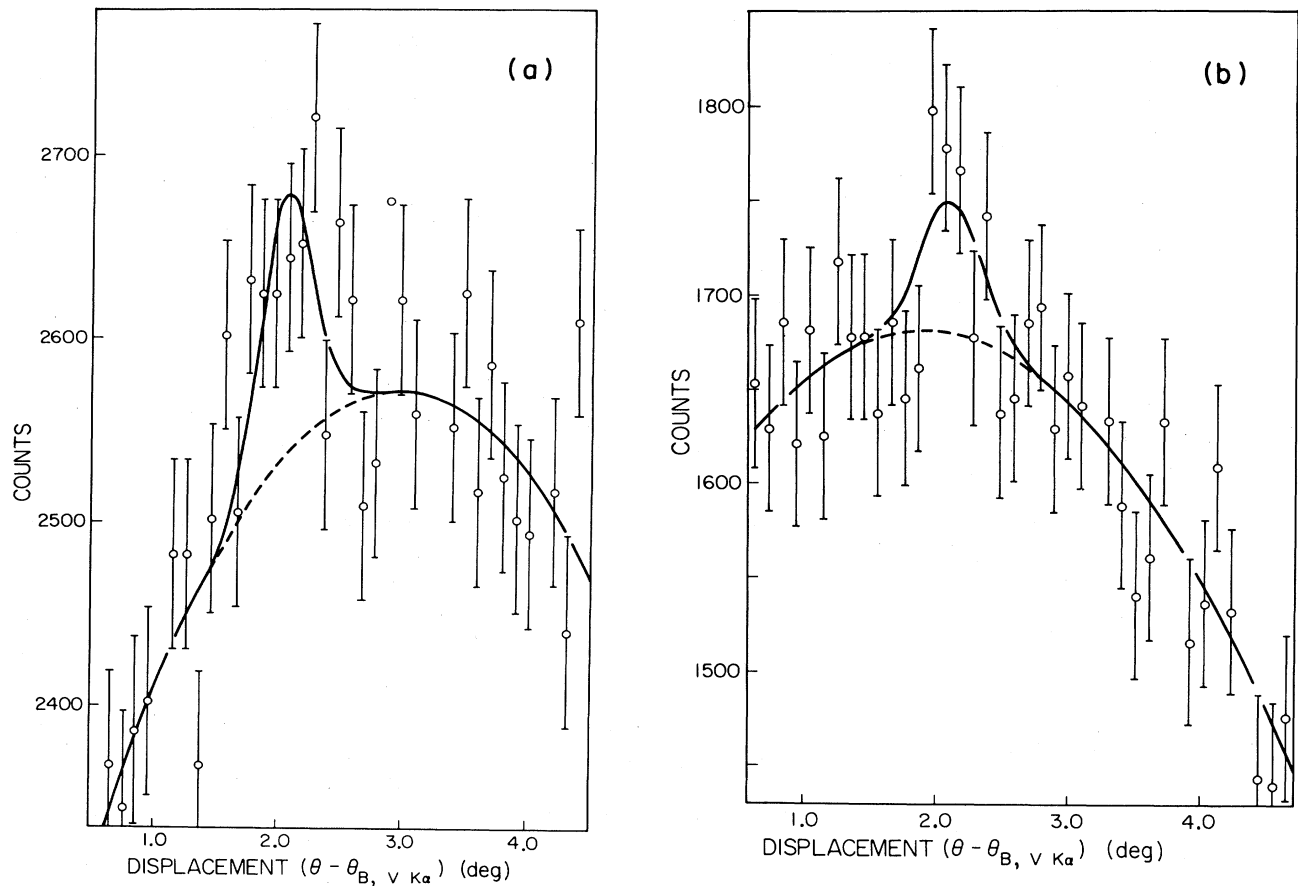


FIG. 7. (a), (b). Pionic hydrogen lines at two different angle settings.

ciency, the signal-to-noise ratio was 1:23. The principal uncertainty in the transition energy thus is statistical. The systematic errors resulting from geometrical uncertainties in the spectrometer arrangement are less than 0.05 eV. Errors arising from the position resolution and a non-linearity of the position sensitive counter are estimated not

to exceed 0.2 eV.

The present results are summarized in Table I. The table also shows our calculated transition energy obtained by solving the Klein-Gordon equation in the Coulomb field for a point nucleus, including the first order vacuum polarization correction. The difference between the Coulomb solution and the measured value constitutes the strong interaction shift of $\epsilon = -3.9 \pm 1.7$ eV.

The preliminary result of Ref. 1, $\epsilon = -12.1 \pm 2.9$ eV, should not be considered to be in conflict with the present value inasmuch as the role of the uncertainties introduced by such factors as the nonlinearity of the position sensitive detector and the reproducibility of the crystal position were underestimated in that reference.

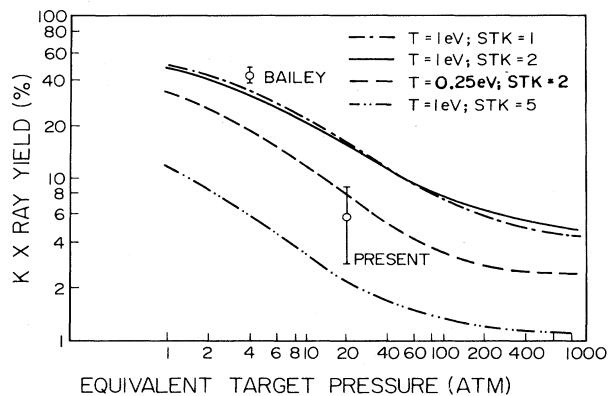


FIG. 8. K x-ray yield as a function of equivalent target pressure at 273 K (Ref. 11).

TABLE I. Energy of the $2p-1s$ transition in eV.

| | |
|--|------------------|
| Measured energy | 2433.5 ± 1.7 |
| Calculated energy (point nucleus) ^a | 2426.4 ± 0.2 |
| Vacuum polarization | 3.2 eV |
| Total | 2429.6 ± 0.2 |
| Strong interaction shift | -3.9 ± 1.7 |

^aRelativistic mass correction included.

The strong interaction shift is related to the s -wave low-energy pion-proton scattering length, $a(\pi^-p)$, by the approximate relation^{16,17}

$$\frac{\epsilon}{|E_{1s}|} = \frac{-4}{r_B} a(\pi^-p),$$

where E_{1s} is the binding energy of the π^- in the $1s$ orbit and r_B is the corresponding Bohr radius. We obtain from our results an s -wave scattering length

$$a(\pi^-p) = 0.070 \pm 0.030 \text{ fm}.$$

The scattering length may be expressed¹⁶ in terms of the isospin components, a_1 (isospin $\frac{1}{2}$) and a_3 (isospin $\frac{3}{2}$), $a(\pi^-p) = (\frac{1}{3})(2a_1 + a_3)$, in order to allow a comparison

with low energy scattering experiments. Results by Orear¹⁸ and by Hamilton and Woolcock¹⁹ yield $a(\pi^-p) = 0.07 \pm 0.02$ and 0.085 ± 0.009 , respectively, in good agreement with our results. The smallness of $a(\pi^-p)$ qualitatively agrees with the approximate calculation by Weinberg.²⁰

ACKNOWLEDGMENTS

Thanks are due to the staff of LAMPF for generous technical support and assistance. The help of J. Markey during the experiment is gratefully acknowledged. One of us (A.F.) wishes to thank the Alexander von Humboldt Foundation for financial support. This work was supported by the US DOE under Contract No. DEAT-0381-ER40002.

*Present address: Physics Department, University of Neuchâtel, Neuchâtel, Switzerland.

†Present address: GEC Hirst Research Centre, Wembley, Great Britain.

¹Eric Bovet *et al.*, Nucl. Instrum. Methods **190**, 613 (1981).

²J. W. Knowles, in *Alpha-, Beta- and Gamma-Ray Spectroscopy*, edited by K. Siegbahn (North-Holland, Amsterdam, 1966), Vol. 1, p. 203.

³*American Institute of Physics Handbook* (McGraw-Hill, New York, 1963), p. 4ff.

⁴R. W. G. Wyckoff, *Crystal Structures*, 2nd ed. (Wiley, New York, 1963), Vol. I.

⁵J. A. Bearden, Rev. Mod. Phys. **39**, 78 (1967).

⁶E. R. Cohen and B. N. Taylor, J. Phys. Chem. Ref. Data **2**, 663 (1973).

⁷A. H. Compton and S. K. Allison, *X Rays in Theory and Experiment* (Van Nostrand, New York, 1947), p. 672ff.

⁸*Handbook of Physics and Chemistry*, edited by R. C. Weast and

M. J. Astle (CRC, Cleveland, Ohio, 1981), p. E-153ff; tables by J. A. Bearden.

⁹R. Kunselman, Ph.D. thesis, University of California Radiation Laboratory Report UCRL-18654, 1969 (unpublished).

¹⁰R. L. Kelly *et al.*, Rev. Mod. Phys. **52**, S44 (1980).

¹¹J. Bailey *et al.*, Phys. Lett. **33B**, 369 (1970).

¹²M. Leon, Phys. Lett. **37B**, 87 (1971).

¹³E. Borie and M. Leon, Phys. Rev. A **21**, 1460 (1980).

¹⁴G. Backenstoss, Annu. Rev. Nucl. Sci. **20**, 467 (1970).

¹⁵G. Rasche and W. S. Woolcock, Nucl. Phys. **A381**, 405 (1982).

¹⁶S. Deser *et al.*, Phys. Rev. **96**, 774 (1954).

¹⁷K. A. Brueckner, Phys. Rev. **98**, 769 (1955).

¹⁸Jay Orear, Phys. Rev. **96**, 176 (1954).

¹⁹J. Hamilton and W. S. Woolcock, Rev. Mod. Phys. **35**, 737 (1963).

²⁰S. Weinberg, Phys. Rev. Lett. **17**, 616 (1966).